Implications of Hemodynamic Forces on Device Stability in Transcatheter Mitral Valve Replacement

Samuel J Hill[1], Ronak Rajani[2], Adelaide De Vecchi[3]

[1]King's College London, London, United Kingdom, SE17 EH

Abstract

In transcatheter mitral valve replacement, a bioprosthetic valve is implanted in the left ventricle to replace a failing native mitral valve. The device landing site is a non-circular annulus that moves and deforms during the cardiac cycle, potentially leading to stability issues that can be aggravated by the forces generated on the bioprosthesis by the blood flow. Furthermore, with the device subjected to high pressure during systole, when the leaflets are closed, late device migration can become a potentially severe complication, especially in cases where the annulus is calcified or following valve-in-valve procedures. To assess the magnitude of ventricular haemodynamic forces during systole, and their correlation with the forces on the device frame, patient-specific computational fluid dynamic (CFD) simulations were performed in 5 transcatheter mitral valve replacement (TMVR) patients.

1. Introduction

Transcatheter valve embolization and migration (TVEM) is a rare, but serious event where the prosthesis dislodges and moves into the left atrium or left ventricle, during or immediately after the procedure. TVEM is associated with a four-fold higher mortality and three-fold higher stroke rate at 30 days' post transcatheter heart valve replacement (Yoon et al., 2019).

The forces exerted by the blood flow on the device play an important role in TVEM. However, TVEM for TMVR is largely undocumented. Reports on Transcatheter Aortic Valve Implantation (TAVI) have shown that TVEM increases the 1-year mortality rate from 14.6% to 38.5% (Kim et al., 2019) and anchoring mitral prosthetics is an even more difficult task. Mitral prosthetics cannot exclusively rely on radial force in the way TAVI devices can, the annular region is shorter, calcification is less reliable, the dynamic motion of the annulus is substantial, and the systolic pressure on the mitral valve reaches up to 120mmHg (Bartorelli et al., 2022).

Predicting migration from pre-procedural datasets is impossible, however using patient-specific imaging data and full 3D computational fluid dynamics simulation (CFD), it is possible to calculate the force acting on the prosthetic from the momentum equation in the Navier-Stokes system. Analysis based on work by Pedrizzetti et al (Pedrizzetti et al., 2017) allows us to infer the heamodynamic force vector (HFV) from wall motion extracted from CT datasets and derive a relationship to the force felt by an implanted prosthetic during systole.

2. Methods

It has been shown that the exchange of forces between the endocardium and the internal fluid can influence pathologies such as the morphogenesis of embryonic hearts and act as a biomarker of mechanical dyssynchrony in heart failure patients (Arvidsson et al., 2017) (Eriksson et al., 2017)**.** The calculation of this force relies on the rate of change of momentum within the ventricular fluid volume, which is balanced by the total haemodynamic forces exerted on that fluid. To compute this, the spatio-temporal velocity field inside the ventricle must be known. These data can be either be derived from 3D echocardiography and 4D flow MRI sequences, which are non-standard in clinical practice, or by performing full three-dimensional CFD simulation based on routine imaging data such as Cine MRI.

Once the internal flow velocity is known the HFV can be calculated using the equation 1 below:

$$\boldsymbol{F}(t) = \rho \int_{V(t)} \left(\frac{\partial \boldsymbol{v}}{\partial t} + \boldsymbol{v} \cdot \nabla \boldsymbol{v} \right) dV \qquad (1)$$

Where **F**(t) is the HFV, ρ is the fluid density, V(t) is the volume and $\boldsymbol{v}$ is the flow velocity.

Full three-dimensional flow simulations are performed using the CFD package STARCCM+ (Siemens PLM). The end-systolic left ventricle endocardium is segmented for each case to create a patient-specific simulation domain in the form of a surface mesh. The endocardium deformation is tracked throughout the cardiac cycle using the medical imaging wall motion tracking software Eidolon (Kerfoot et al., 2016).

The surface and volume integrals were calculated using STARCCM+ field functions, the time derivative of velocity was evaluated across the boundary and the entire domain respectively.

The force experienced by the frame of the bioprosthesis is calculated as a surface integral of the pressure field over

that surface. The angle θ between the vertical axis of the prosthetic and the direction of the HFV was calculated from the ventricular anatomy (Fig 1).

Figure 1 - Angle between the prosthesis axis and HVF direction in a systolic frame. The altered shape of the left ventricular out flow tract (neo-LVOT) after implantation is also shown in red..

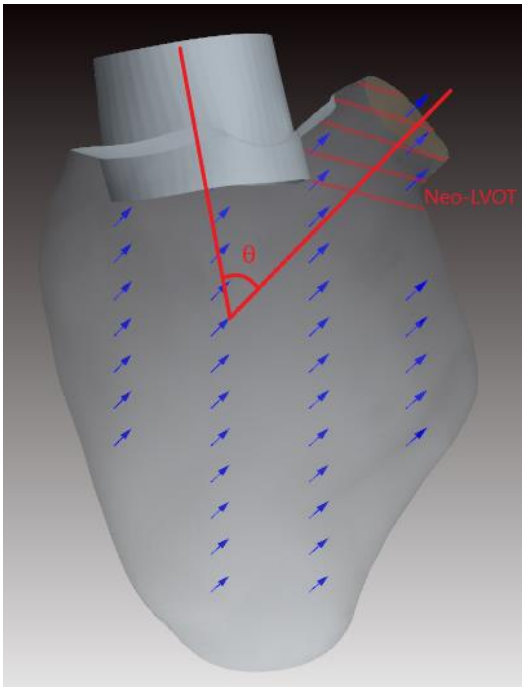

2.1. Patients

Five male patients candidate for TMVR (67.6±8.63 years) were included in this study . The ejection fraction of the patients is 30.57±5.06% and the heart rate is 64.41±10.45 bpm. The end-systolic volume and end-diastolic volumes had an average of 167.7±21.3ml and 243.6±40.9ml respectively.

2.2. Image Processing

Segmentation of the LV blood pool was performed using MITKWorkbench (Mint Medical). After embedding the CAD model of the bioprosthetic device into the LV mesh, the left ventricular outflow tract (LVOT) reduced area was measured. TMVR often results in a change of shape and size of the LVOT due to device protrusion inside the ventricular cavity, which creates a narrower passage (neo-LVOT) seen as the shaded region in Figure 1. To ensure patient-specificity and validate the anatomical model, the LV length, diameter, aortomitral angle and septal distance are compared from CT to simulation domain (Figure 2). Mean and standard deviation are 86.58±6.48mm for the LV length, 45.22±8.52mm for the LV diameter, 120.19±10˚ for the Aortomitral angle and 33.84±3.05mm for the septal distance.

Wall motion tracking was performed using a temporally sparse free-form deformation algorithm and prescribed on the endocardial boundary of the model. From the volume change, the inflow and outflow velocity at the valve boundaries were also calculated. LV length, diameter, aortomitral angle and septal distance measurements were taken again at each time interval to validate against image-derived measurements.

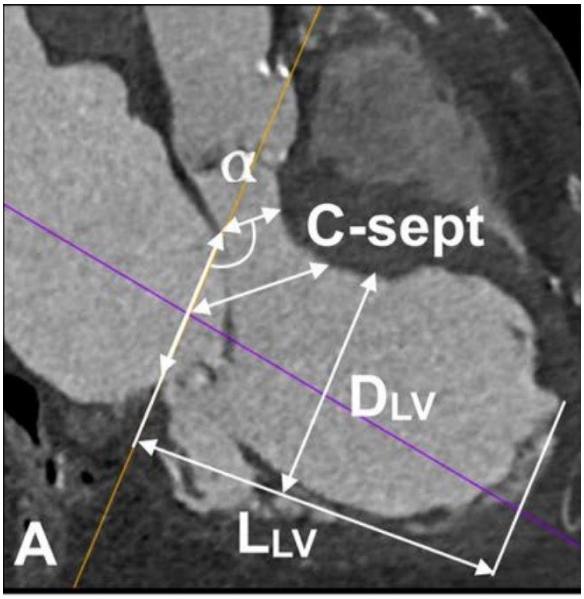

Figure 2 - LV Measurements

2.3. Hemodynamic Force Vector Calculations

The contribution of the HFV acting on the prosthetic device shown in grey in Figure 1 can be resolved in either the longitudinal vertical axis or the horizontal, i.e. the basal-apical and inferior-anterior direction respectively (Eq. 1). The longitudinal contribution along the former would impact the migration of the device to or from the LV into the left atrium (LA). During systole the pressure builds in the LV and insufficient anchoring of the prosthetic can lead to migration with catastrophic consequences.

The horizontal projection of the HFV acts sideways on the device frame, with potential to affect its stability, with potential undesirable effects such as paravalvular leakage, a well-recognised complication. Although it is a rare occurrence in patients with a non-calcified mitral orifice, this is frequently observed in cases of mitral annular calcification (De Backer et al., 2014).

$$Fv = HFV * \cos\theta \qquad Fh = HFV * \sin\theta \quad (2)$$

The HFV vector was normalised based on the ejection fraction to allow for comparison between patients.

3. Results

The normalised HFV has a maximum of 2.94N with average 1.48±0.79N. The maximum force observed was 10.94N, the average was 4.37±3.69N.

Figure 3 shows the distribution of endocardium contraction patterns prior to peak systole for Patients 1 (panels A,C) and 4 (panels B,D). Patient 1 has a lower average displacement per timestep at 1.54e-5m per millisecond, whereas patients 4 has a larger average at 1.73e-5m. Patient 4 also has a large patch of high values near the apical region reaching 2.6e-5m, whereas Patient 1 has areas of high displacement near the basal region in the anterior wall.

The HFV was plotted against the average force on the valve surface showing as expected a strong correlation, as shown in Figure 4. When resolved in both the basal-apical and inferior-anterior directions the correlation was also strong with r^2 values 0.92 and 0.98 respectively (Figure 5-6). The lowest of these values is the basal-apical dataset due to the high basal-apical contribution of Patient 4.

Patients 1, 2, 3 and 5 showed a relatively low force acting on valve, with patient 1 exhibiting the lowest at 0.41N. Patient 4 showed a significantly higher force on valve at 10.94N. As patient 4 has the highest HFV when resolved in the both directions, they would therefore be at greatest risk of both valve migration and paravalvular leakage.

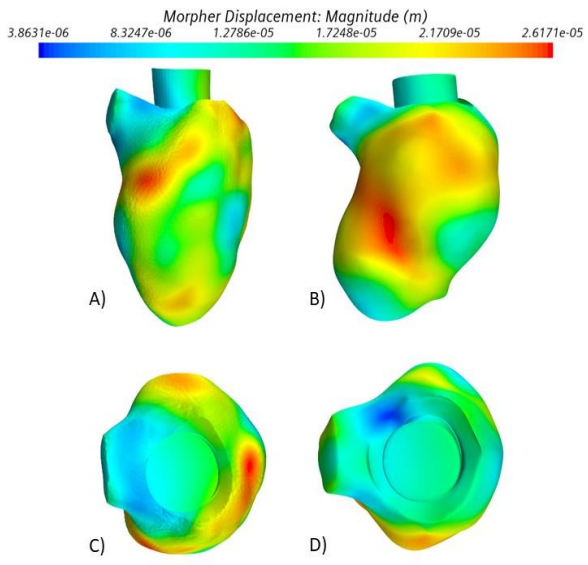

Figure 3 - Contraction patterns for patients 1 (A,C) and,4 (B,D)

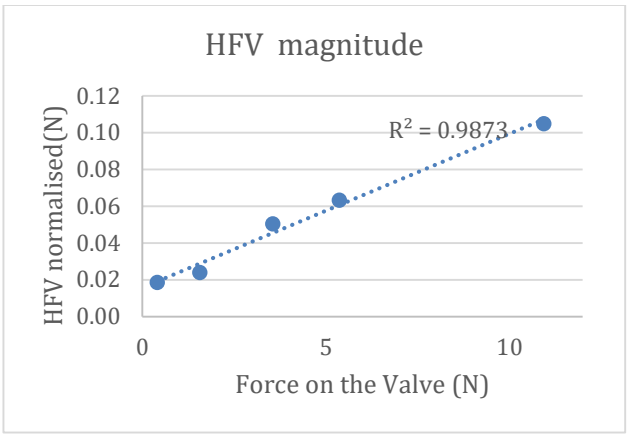

Figure 4 - HFV magnitude normalised by the ejection fraction and plotted vs the force acting on the valve for each patient

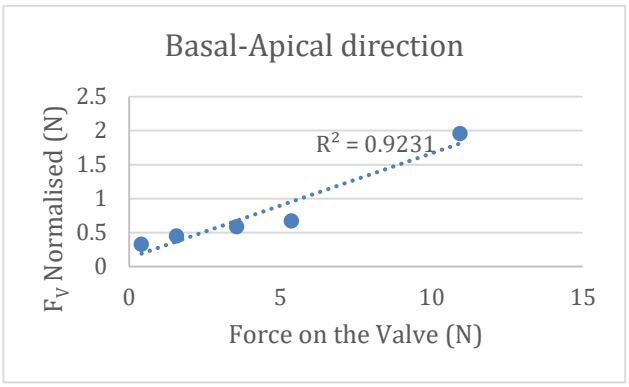

Figure 5 – Normalised HFV projected in the basal-apical direction

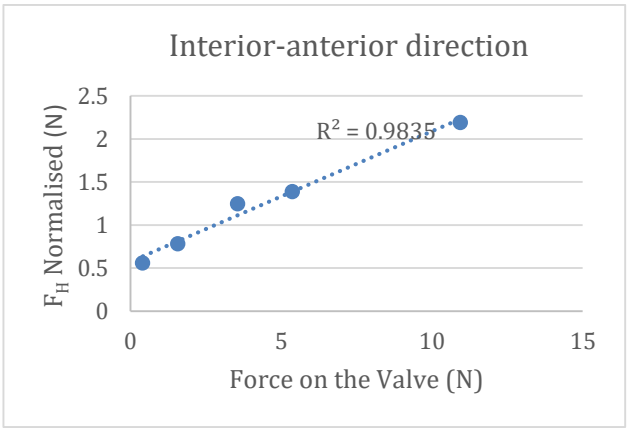

Figure 6 – Normalised HFV projected in the interior-anterior direction

4. Discussion

The results presented show a clear correlation between the magnitude of the HFV and the force felt by the prosthetic

device. Patient 4 is of particular interest in this set of results. The contraction pattern indicates a large region of endocardial movement, which corresponds with an observed large HFV. This area is also near the apical region of the ventricle and its displacement points towards the base, therefore contributing predominantly to the basal-apical component of the HFV. Patient 4 also has the smallest θ angle. The direction of the HFV, which is usually aligned with the left ventricular outflow tract, would then also have a higher basal-apical component than its interior-anterior counterpart. This configuration requires the blood flow being ejected to re-align with the neo-LVOT, resulting in energy dissipation and a less efficient ejection. When observing the trend-line for the basal-apical component, Patient 4 has a higher value than the rest of the cohort. Device stability concerning valve migration would therefore be much more a concern for this patient than others. In contrast Patient 1 exhibits a contraction pattern that is more aligned to the anterior-posterior direction, with largest values of displacement in at mid-ventricle and in the basal region, where Patient 4 exhibits almost zero motion. This suggests that the ventricle is able to eject the flow in the upper half of the cavity, while the apical region exhibits lower flow velocities.

This type of analysis shows the potential to predict the haemodynamic force distribution from the endocardial motion, which can be derived from standard Cine-MRI sequences. This can be demonstrated mathematically from equation (1) using the divergence theorem and mass conservation. Adding non-invasive estimation of haemodynamic forces on the device to pre-procedural assessment could provide critical information on the suitability of interventions involving risks of valve migration such as valve-in-valve procedures.

5. Limitations

The sample size is limited to five patients due to the availability of quality CT datasets without the presence of artefacts. The CFD model is limited by the approximation of the prosthetic model to a real device – no device leaflets present and the device frame is idealised. The endocardium model has been smoothed and papillary muscles removed to aid in the numerical stability during simulation.

Acknowledgments

This research was supported by the EPSRC [EP/R513064/1].

References

Arvidsson, P. M., Töger, J., Carlsson, M., Steding-Ehrenborg, K., Pedrizzetti, G., Heiberg, E., & Arheden, H. (2017). Left and right ventricular hemodynamic forces in healthy volunteers and elite athletes assessed with 4D flow magnetic resonance imaging. *American Journal of Physiology. Heart and Circulatory Physiology*, *312*(2), H314–H328. https://doi.org/10.1152/AJPHEART.00583.2016

Bartorelli, A. L., Monizzi, G., Mastrangelo, A., Grancini, L., Fabbiocchi, F., Conte, E., … Andreini, D. (2022). Transcatheter mitral valve replacement: there is still work to be done. *European Heart Journal Supplements*, 16–21. https://doi.org/10.1093/eurheartjsupp/suac098

De Backer, O., Piazza, N., Banai, S., Lutter, G., Maisano, F., Herrmann, H. C., … Søndergaard, L. (2014). Percutaneous transcatheter mitral valve replacement: An overview of devices in preclinical and early clinical evaluation. *Circulation: Cardiovascular Interventions*, Vol. 7, pp. 400–409. https://doi.org/10.1161/CIRCINTERVENTIONS.114.001607

Eriksson, J., Zajac, J., Alehagen, U., Bolger, A. F., Ebbers, T., & Carlhäll, C. J. (2017). Left ventricular hemodynamic forces as a marker of mechanical dyssynchrony in heart failure patients with left bundle branch block. *Scientific Reports*, *7*(1). https://doi.org/10.1038/S41598-017-03089-X

Kerfoot, E., Fovargue, L., Rivolo, S., Shi, W., Rueckert, D., Nordsletten, D., … Razavi, R. (2016). Eidolon: Visualization and computational framework for multi-modal biomedical data analysis. *Lecture Notes in Computer Science (Including Subseries Lecture Notes in Artificial Intelligence and Lecture Notes in Bioinformatics)*, *9805 LNCS*, 425–437. https://doi.org/10.1007/978-3-319-43775-0_39

Kim, W. K., Schäfer, U., Tchetche, D., Nef, H., Arnold, M., Avanzas, P., … Hamm, C. W. (2019). Incidence and outcome of peri-procedural transcatheter heart valve embolization and migration: The TRAVEL registry (TranscatheteR HeArt Valve EmboLization and Migration). *European Heart Journal*, *40*(38), 3156–3165. https://doi.org/10.1093/eurheartj/ehz429

Pedrizzetti, G., Arvidsson, P. M., Töger, J., Borgquist, R., Domenichini, F., Arheden, H., & Heiberg, E. (2017). On estimating intraventricular hemodynamic forces from endocardial dynamics: A comparative study with 4D flow MRI. *Journal of Biomechanics*, *60*, 203–210. https://doi.org/10.1016/j.jbiomech.2017.06.046

Yoon, S. H., Whisenant, B. K., Bleiziffer, S., Delgado, V., Dhoble, A., Schofer, N., … Makkar, R. R. (2019). Outcomes of transcatheter mitral valve replacement for degenerated bioprostheses, failed annuloplasty rings, and mitral annular calcification. *European Heart Journal*, *40*(5), 441–451. https://doi.org/10.1093/EURHEARTJ/EHY590

Address for correspondence:

Samuel J Hill.
School of Biomedical Engineering and Imaging Sciences, King's College London, St Thomas' Hospital, London, SE1 7EH, UK.
Samuel.hill@kcl.ac.uk